Deep-Sea Research II 58 (2011) 378–386

Contents lists available at ScienceDirect

Deep-Sea Research II

journal homepage: www.elsevier.com/locate/dsr2

Nanoplankton mixotrophy in the eastern equatorial Pacific

Michael R. Stukel [a,*], Michael R. Landry [a], Karen E. Selph [b]

[a] Scripps Institution of Oceanography, University of California at San Diego, La Jolla, CA 92093-0227, USA
[b] Department of Oceanography, University of Hawaii at Manoa, Honolulu, HI 96822, USA

ARTICLE INFO

Article history:
Received 9 August 2010
Accepted 9 August 2010
Available online 26 August 2010

Keywords:
Mixotrophy
Phagotrophy
Nanoplankton
Equatorial Pacific
Microzooplankton grazing
HNLC

ABSTRACT

Heterotrophic bacteria, cyanobacteria, and picoeukaryotic algae dominate the plankton community of high nutrient-low chlorophyll (HNLC) areas of the eastern equatorial Pacific (EEP). While grazing on these picoplankton is often attributed to aplastidic zooflagellates, mixotrophic nanoflagellates (phagotrophic phototrophs) may also exert a large grazing pressure. We assessed the relative contributions of mixotrophic nanoplankton and obligate heterotrophs to picoplankton phagotrophy in mixed-layer water of the EEP using 0.8-μm Fluorescently-Labeled Bacteria (FLB). Obligate heterotrophs and phototrophs were distinguished from their ratios of microscopically measured red (chlorophyll *a*) to green (proflavin-stained protein) fluorescence. Sampling sites were located along a nutrient gradient formed by a tropical instability wave at 0.5°N between 123.5°W and 128°W and at 1.75°N, 125°W. The majority of ingested particles were found within 3-5 μm flagellates, with 54% of the demonstrated phagotrophs belonging to the high-pigment putatively phototrophic population and obligate heterotrophs responsible for 51% of the demonstrated phagotrophy due to their greater propensity to ingest multiple prey. The importance of mixotrophy as a means of alleviating nutrient stress is indicated by a strong inverse relationship between the proportion of community FLB uptake by mixotrophs and ambient nutrient concentration. Low ambient Fe concentration and a demonstrated community response to Fe-addition in shipboard grow-out experiments suggest that mixotrophs were primarily engaging in phagotrophy to offset Fe-deficiencies.

1. Introduction

Phagotrophic mixotrophy is a common nutritional strategy in the pelagic realm (Jones, 2000; Sanders, 1991), and can be found in most taxa of eukaryotic phytoplankton, with the notable exception of diatoms. The incredible diversity of mixotrophs, as well as their numerical abundance in many regions, suggests that they may play an important role in the cycling of nutrients and organic matter in the euphotic zone. However, they are frequently ignored in ecosystem studies, while all protistan bacterivory and herbivory are attributed to aplastidic (heterotrophic) cells.

Mixotrophy allows nutritional flexibility, but it comes with an associated cost of the manufacture of both photosynthetic and phagotrophic apparatus. Raven (1997) showed that the cost (in terms of energy, C, N, and Fe) of synthesis of photosynthetic machinery is typically 50% of total cellular synthesis while the corresponding synthesis cost of phagotrophy is $<10\%$. Thus, when considering maximal growth capacities, mixotrophy requires an increased cost of manufacture of cellular machinery relative to obligate phototrophs or heterotrophs. However, the resulting nutritional plasticity may allow mixotrophs to outcompete co-occurring nutritional specialists when prey or nutrients are limiting (Nygaard and Tobiesen, 1993; Raven, 1997).

Although facultative phagotrophy has been shown to allow phytoplankton to survive light-limiting conditions by obtaining carbon from prey cells (e.g. Bell and Laybourn-Parry, 2003; Caron et al., 1993), a growing consensus suggests that mixotrophs in the open ocean rely more on phagotrophy as a strategy for alleviating nutrient stress. Mixotrophs that obtain most of their carbon from photosynthesis can supplement dissolved nitrogen uptake by ingesting protein-rich picoplankton (e.g. Arenovski et al., 1995; Nygaard and Tobiesen, 1993). Similarly, Fe-deficient phototrophs can efficiently assimilate Fe from ingested bacteria (Maranger et al., 1998). In both cases, larger nanophytoplankton that would fare poorly when competing against picophytoplankton for dissolved nutrients in low nutrient systems are able to cull resources from smaller plankton with high specific uptake rates. Although these laboratory experiments suggest an important role for mixotrophic nutrition in oligotrophic regions, most studies of phagotrophic capabilities in marine habitats have focused on coastal regions (e.g. Baretta-Bekker et al., 1998; Havskum and Hansen, 1997; Nygaard and Tobiesen, 1993; Unrein et al., 2007) while only a handful have occurred in the remote oligotrophic regions (e.g. Arenovski et al., 1995; Safi and Hall, 1999; Sanders

* Corresponding author. Tel.: +1 8585244909; fax: +1 8585346500.
E-mail address: mstukel@ucsd.edu (M.R. Stukel).

0967-0645/$ - see front matter © 2010 Elsevier Ltd. All rights reserved.
doi:10.1016/j.dsr2.2010.08.016

et al., 2000; Zubkov and Tarran, 2008) that comprise the majority of the ocean's surface.

Mixotrophs may play a critical, although currently uncharacterized, role in high nutrient-low chlorophyll (HNLC) regions where fluctuations in autotrophic biomass are dampened by low nutrient uptake rates of Fe-deficient large phytoplankton (e.g. Franck et al., 2003; Franck et al., 2005) and high grazing rates on pico- and nanoplankton (e.g. Le Borgne and Landry, 2003). Phagotrophy on the abundant populations of picoplankton may provide a reliable source of Fe for larger mixotrophs. Additionally, phagotrophy could alleviate nutrient stress in high nitrate waters where eukaryotic phytoplankton often rely on recycled production, since nitrate uptake rate is depressed in Fe-deficient cells (Franck et al., 2003).

High rates of phagotrophy by nanoplanktonic phototrophs may also help explain the tight coupling of picoplanktonic growth and grazing rates that is typically found in HNLC and oligotrophic systems (Miller et al., 1991). Substantial phagotrophy by phototrophs would significantly increase the grazer pool and therefore the potential grazing pressure exerted on smaller plankton. At the same time, mixotrophs that rely only peripherally on consuming prey would not have typical predator-prey dependencies and experience the out of phase population fluctuations that can result (Jost et al., 2004).

The Eastern Equatorial Pacific (EEP) is an open-ocean region where growth of large autotrophs is strongly limited by low levels of dissolved Fe (Coale et al, 1996b; Landry et al., 2000a). Hence, it is an area where photosynthetically-capable flagellates might find advantages to functioning as facultative phagotrophs, consuming Fe-rich bacteria and picoautotrophs. As part of a 2005 study of phytoplankton control mechanisms in the equatorial Pacific, we conducted uptake experiments with fluorescently labeled bacteria (FLB) to characterize the size structure and trophic status of nanoflagellates that can feed on cells in picoplankton size range. These particles were used as proxies for the *Prochlorococcus*, *Synechococcus*, picoeukaryotes and heterotrophic bacteria that dominate the open ocean (Landry and Kirchman, 2002). The use of chlorophyll fluorescence differences within FLB-ingesting cells allowed us to objectively characterize the pigmentation of phagotrophic nanoflagellates and separate the community into plastidic and aplastidic cells. Mixed-layer samples were taken within and adjacent to a tropical instability wave (TIW) to assess the role of nutrient supply on the relative importance of bacterivory by mixotrophs and obligate heterotrophs. TIWs are areas of increased circulation and therefore may be associated with increased nutrients relative to surrounding surface waters (Barber et al., 1996; Foley et al., 1997; Strutton et al., 2001). The prevailing paradigm that nanoplanktonic mixotrophs typically consume bacterial prey to acquire nutrients (Legrand et al., 1998; Maranger et al., 1998; Nygaard and Tobiesen, 1993) would suggest that plastidic cells should form a lesser component of the phagotrophic community within the higher nutrient regime of a TIW. The relative importance of phagotrophy was also expected to increase with the reduced surface area to biovolume ratios of larger phytoplankton, due to their decreased capacity to utilize dissolved nutrients relative to picophytoplankton.

2. Materials & methods

2.1. Sample collection

Our study was conducted in the equatorial Pacific onboard the *R/V Roger Revelle* during late September 2005. One-liter samples were collected from 18-m depth, which is representative of the mixed-layer where phytoplankton carbon biomass and specific growth and grazing rates were highest (Selph et al., 2011; Taylor et al., 2011). Samples were taken at four stations in the equatorial Pacific (0.5°N, 128°W; 0.5°N, 125.7°W; 0.5°N, 123.5°W; and 1.75°N, 125°W) that spanned a TIW, with the first two stations representing higher nutrient input within the TIW and the second two representative of the lower nutrient input. The TIW could be clearly seen in satellite images of sea surface temperature as a northward excursion of cold equatorial water that propagated to the west during the cruise (Strutton et al., 2011). Although mixed-layer concentrations of dissolved Fe remained low across the TIW, nitrate concentrations, indicative of increased vertical mixing, increased from 4.3 μM on the periphery to 7.8 μM within the TIW core.

2.2. Incubations with Fluorescently-Labeled Bacteria (FLB)

Heat-killed fluorescently-labeled bacteria (FLB) were prepared using the method of Sherr et al. (1987) from a natural marine isolate (~0.8-μm diameter) grown to late exponential growth phase in seawater L-broth. Aliquots of FLB were stored frozen, then thawed, vortexed and pre-filtered through a 2-μm filter to eliminate clumps prior to use. While the FLB used cannot be considered universal surrogates for the diverse array of heterotrophic bacteria and picophytoplankton, which vary in size, shape, and cell surface characteristics, the grazing rate estimates from simultaneous use of FLB-disappearance and the dilution method in the equatorial Pacific have shown good agreement, suggesting that FLB are consumed similarly to natural picoplankton (Landry et al., 1995).

For FLB-uptake experiments, seawater samples were collected at night and allowed to acclimate to bottle containment (1-L polycarbonate) for up to 12 hours in shipboard incubators maintained at ambient light levels (31% surface irradiance) and cooled with mixed-layer seawater. FLB were added to the bottles at a target concentration of ~80,000 mL^{-1} and dispersed by gentle mixing, and initial (t=0) samples of 100 mL were taken as a blank to assure that coincidental FLB-flagellate contact not associated with phagotrophy was insignificant. After 60 min incubations, final subsamples (100 mL) were taken to assess the community composition and the characteristics of cells with ingested FLB (i.e. demonstrated phagotrophy). Given the elevated temperatures of the equatorial waters (~24 °C), the one-hour incubations were considered sufficient for uptake rates to come into balance with digestion and vacuole egestion rates (Sherr et al., 1988), giving steady state maximal ratios of FLB per cell for the given experimental conditions.

2.3. Epifluorescence microscopy

Initial and final 100 mL microscopy samples were fixed by sequential addition of 100 μL alkaline Lugol's solution (0.1%, final concentration), 1 mL 10% formalin, and 300 μL 3% sodium thiosulfate (protocol modified from Sherr and Sherr, 1993). Samples were then briefly stained with 80 μL 0.033% (w/v) proflavin (a protein stain) and 250 μL of the nucleic acid stain DAPI (50 μg mL^{-1}, final concentration) and filtered onto 25-mm black Nuclepore polycarbonate filters with 2-μm pore size. The filters were mounted with immersion oil onto glass slides and frozen at −80 °C for laboratory analysis.

Slides were analyzed with a Zeiss inverted epifluorescence microscope at 630X magnification. For each slide, 75 random fields were imaged with an attached CCD camera and three filter sets: A blue long-pass (FITC) set (excitation wavelengths: 450-490 nm; emission: >515 nm), a chlorophyll *a* filter set (excitation: 465-495 nm; emission: 635-685 nm), and a UV

(DAPI) filter set (excitation: 340-380 nm; emission: 435-485 nm). Each imaged field was inspected manually under the microscope to identify FLB-containing cells (FLB were visible as bright green spheres under the FITC filter set) and their locations on the digital field. Images were analyzed using Image Pro software. Nanoplankton cells (excluding diatoms, which were assumed incapable of phagotrophy) were manually segmented (to determine two-dimensional cell size and shape) based on luminosity in the FITC and chlorophyll *a* filter set and the presence of an identifiable nucleus in the DAPI channel. Densitometric mean gray values in each 8-bit color channel were calculated for each cell as well as area and the maximum caliper length. Cells with a maximum caliper length less than 2 μm were eliminated based on the assumption that they would not be quantitatively collected on a 2-μm pore size filter. The mode background grey value of each image was subtracted from each cellular densitometric mean, and each image was normalized to a standard exposure time to ensure consistent fluorescence values across images. Area and maximum caliper length were converted to biovolume (BV) and equivalent spherical diameter (ESD) by assuming a prolate spherical shape. Biomass of the community (excluding diatoms) was calculated assuming a carbon to biovolume relationship of pg C $cell^{-1} = 0.216 \times BV^{0.939}$ (Menden-Deuer and Lessard, 2000).

2.4. Statistical comparisons of populations

Cells from each sample were pooled, and a histogram was plotted in log-space of the normalized ratio of red fluorescence (chlorophyll) to green fluorescence (proflavin-stained protein). The distinct bi-modal shape of the curve indicated the presence of two separate communities and allowed us to distinguish high-pigment from low-pigment cells (see section 3.1). Similar histograms from each sample were compared to ensure that the cutoff between low- and high-pigment cells was consistent between stations.

Cell-size abundance plots were created by binning nanoplankton cells into logarithmic size classes (Sabetta et al., 2005). Normalized Biomass-Size (NB-S) spectra were created to objectively compare size distributions of different nanoplankton populations. They were constructed by taking the logarithms of biomass sums of all cells within octave scales of 5 cellular carbon size classes and dividing by the size class intervals (Martin et al., 2006; Platt and Denman, 1977). The smallest size class began at a cellular carbon level equivalent to 2-μm ESD. The relative dominance of large and small cells within samples was determined by computing the slope of a line fit to the NB-S spectrum: $B_m/\Delta m = am^b$, where B_m is the population biomass of a size class, m is the mean of the size class, Δm is the size class interval, and a and b are constants.

3. Results

3.1. Determination of high-pigment and low-pigment cells

When quantified in terms of the ratios of their microscope-based red:green fluorescence, the nanoplankton assemblage exhibited a bimodal distribution, but with an ambiguous division between the high-pigment and low-pigment forms (Fig. 1A). The low-pigment cells are assumed to exhibit a primarily heterotrophic nutritional strategy, while the high-pigment cells can be classified as functionally photosynthetic. We defined a cutoff for separating low- and high-pigment cells as the local minimum in the probability density function of the ratio of red:green fluorescence as shown for the pooled samples in Fig. 1. Histograms of red:green fluorescence for each station (not shown) were examined to ensure that this cutoff was consistent for all samples despite changes observed in nutrient concentration and a shift in the dominant nanoplankton within the TIW (Selph et al., 2011; Taylor et al., 2011).

Our empirical separation of low- and high-pigment cells divided the pooled (all stations) nanoplankton community of 9,034 cells into 67% high-pigment phototrophs and 33% low-pigment obligate heterotrophs. When scaled by biomass, high-pigment cells (excluding diatoms) comprised 74% of the nanoplankton biomass in the samples. The red:green fluorescence threshold from the nanoplankton assemblage at large was then applied to the 228 cells that contained FLB which divided the FLB-ingesting community into 54% high-pigment phagotrophs and 46% low-pigment phagotrophs (Fig. 1B). Given the 2-fold higher concentrations of high-pigment nanoflagellates in the community, a lower proportion of them exhibited phagotrophic behavior compared to obligate heterotrophs, but their contribution to total community predation on picoplankton-sized prey was nonetheless substantial.

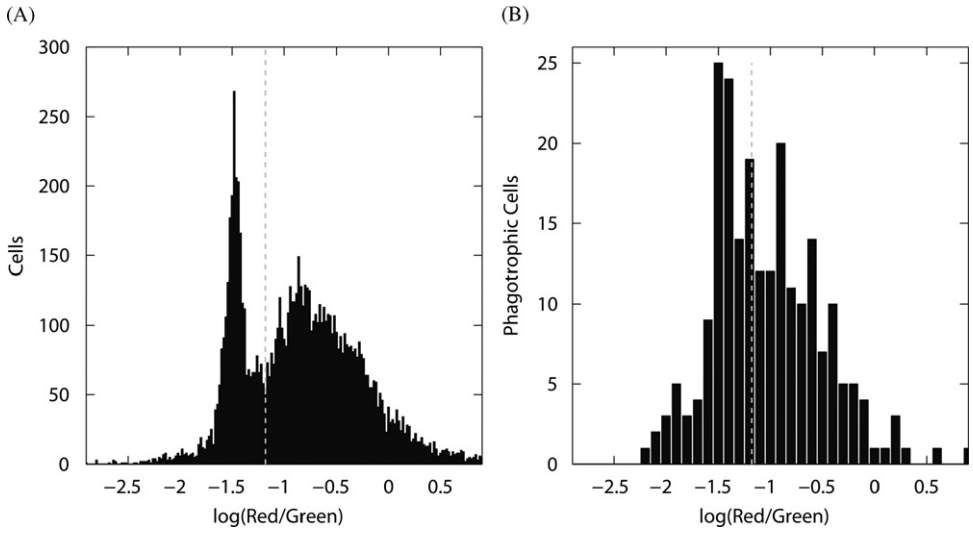

Fig. 1. Ratio of red:green fluorescence used to distinguish high-pigment (phototrophic) cells from low-pigment (obligate heterotrophic) cells. (A) Histogram displaying the logarithm of red (chlorophyll *a*) to green (proflavin) fluorescence for all cells imaged. The dashed line shows the division between high- and low-pigment cells that we objectively defined as the local minimum in the probability density function. (B) Histogram of the logarithm of red (chlorophyll *a*) to green (proflavin) for the subset of the population with ingested FLB.

Additionally, the low-pigment cells in our phagotrophic (FLB-containing) subset had a higher red:green fluorescence than the general assemblage of low-pigment cells, with a large proportion exhibiting a red:green fluorescence ratio that was close to our objectively-defined heterotroph:phototroph cutoff (Fig. 1B).

3.2. Size spectra

Fig. 2A shows a cell-size abundance distribution for all nanoplankton cells in the four pooled samples. The pattern resembles the normal distributions typically found in populations except for a broad shoulder in the 3-4 μm range and our undersampling of the smallest size classes with the 2-μm filters. The mode in the size distribution equates to an ESD of 2.14 μm. The FLB-ingesting subset of the population (Fig. 2B) has a significantly larger modal ESD of 3.40 μm, implying that the average phagotroph was larger than the mean cell size in the assemblage. The predominant role of 3-4 μm cells in phagotrophy on 0.8-μm particles is in excellent agreement with the 4-fold size relation between nanoflagellates and their bacterial prey shown experimentally by Calbet and Landry (1999). It is also consistent with the

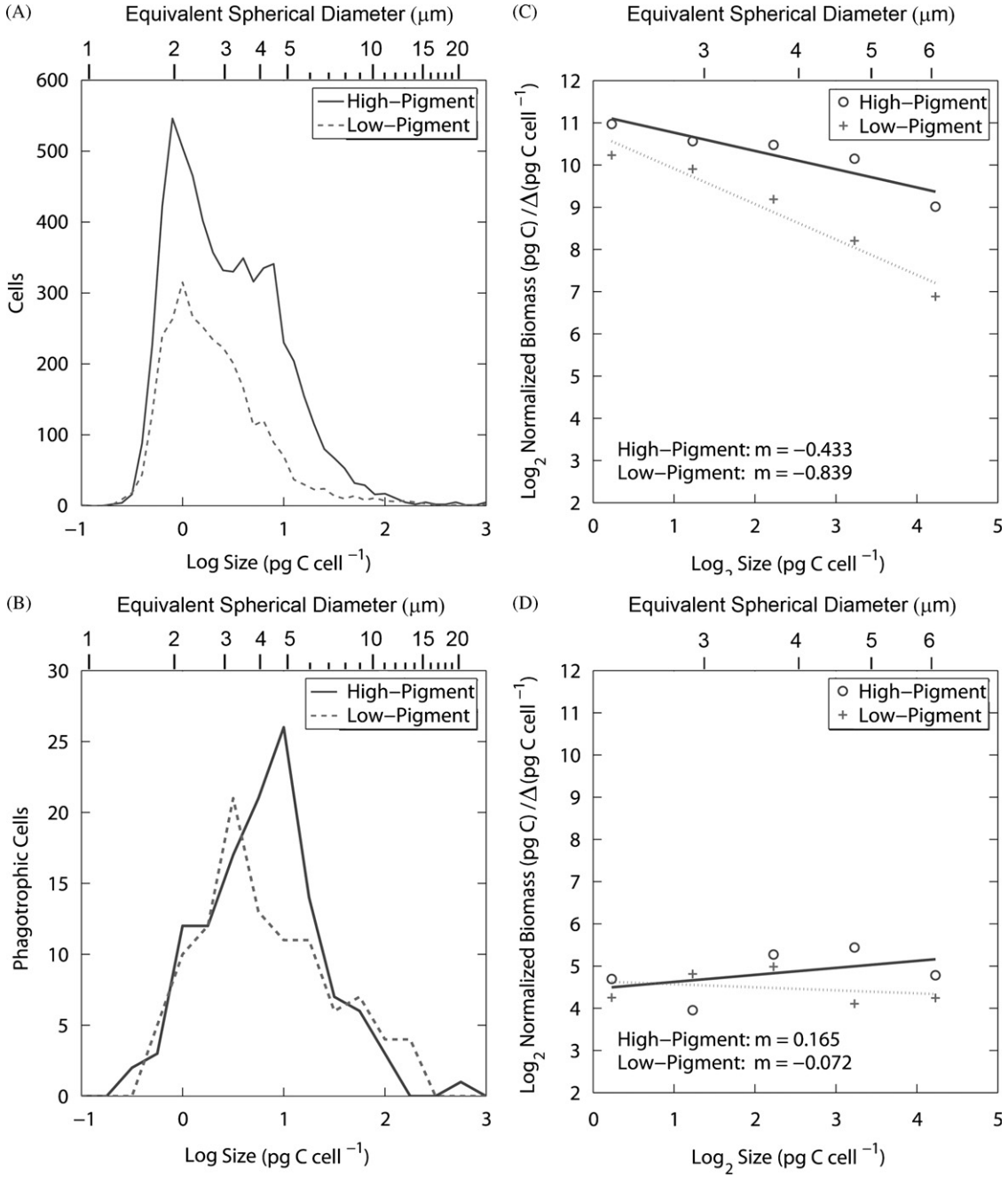

Fig. 2. Size distributions of nanoplankton in the eastern equatorial Pacific. (A) Cell size abundance plot (Sabetta et al., 2005) of all nanoplankton. Cells were binned into logarithmic size classes based on their calculated carbon content per individual. Y-axis is the abundance of each size class. The upper x-axis shows the equivalent spherical diameter for a cell of the appropriate carbon content. (B) Same as a, but plotted for the high-pigment phagotrophic subset (solid line) and the low-pigment phagotrophic subset (dashed line). (C) Normalized Biomass-Size (NB-S) spectra for all high-pigment (circles, solid line) and low-pigment (plus symbols, dotted line) nanoplankton. Cells were binned in an octave scale based on cellular carbon content per individual. Y-axis is the biomass of a particular size class. Larger (positive) slopes indicate a greater proportion of large cells in the sample (Martin et al., 2006; Platt and Denman, 1977). Again, the upper x-axis shows the equivalent spherical diameter. (D) Same as c but plotted for the phagotrophic subset.

general observation that <5-μm flagellates are responsible for the majority of grazing pressure on picoplankton (see review by Sherr and Sherr, 2002). A comparison of the cell-size abundance distributions of high-pigment and low-pigment phagotrophs shows that while the modal size of high-pigment cells is larger than for low-pigment cells, there are more >10-μm low-pigment cells on the tail of the distribution than high-pigment phagotrophs. The slopes of the NB-S spectra (Fig. 2C,D) allow us to assess the relative contributions of large and small nanoplankton cells to each population. It is clear from the diagrams that large cells (>5-μm) are relatively more abundant in the high-pigment sample for both the total nanoplankton assemblage and the phagotrophic subset. While this supports our expectation that mixotrophs should be larger in size than obligate heterotrophs because >5-μm phytoplankton have lower nutrient uptake rates than smaller phototrophs and hence a greater need to ingest prey to alleviate nutrient stress, the small sample size of the phagotrophic subset leads to a poor fit between the data and the regression line.

3.3. Tropical Instability Wave

Typically Fe and nitrogen inputs to the surface ocean are decoupled; although nitrate is primarily introduced through upwelling, the supply of upwelled Fe is insufficient for phytoplankton growth requirements and is usually supplemented by significant inputs to the system from aeolian deposition. In the HNLC region of the equatorial Pacific, however, the primary source of Fe is upwelled equatorial undercurrent water which supplies both nitrate and Fe (Coale et al., 1996a). Thus, while an anticipated increase in mixed-layer dissolved Fe was not observed in the TIW, a significant elevation of nitrate (8 μM) was measured (Strutton et al., 2011), suggesting an increased input rate of both macro- and micronutrients from the TIW effect on shoaling isopycnals. Elevated chlorophyll *a* concentrations within the TIW (Selph et al., 2011), further suggest increased Fe input, which may have been rapidly taken up by the Fe-limited plankton community. Fe-enrichment experiments in the equatorial Pacific (Coale et al., 1996b; Landry et al., 2000b) have shown that the initial community response to increased Fe inputs is a rapid increase in the Chl *a*:carbon ratio, with a concomitant biomass response that only follows days later. Similarly, our samples in the TIW showed elevated Chl *a* concentrations without a significant increase in phytoplankton biomass (Selph et al., 2011; Taylor et al., 2011), which may be a response to decreased Fe-deficiency or an uplifting of cells adapted to lower light levels.

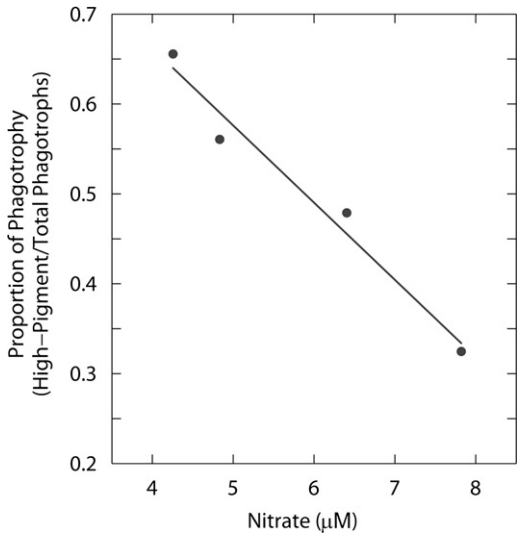

Fig. 3. Correlation of mixotrophic phagotrophy with ambient dissolved nitrate concentration. Y-axis is the ratio of the FLB ingestion rate by high-pigment cells to the total measured FLB ingestion rate within a sample. The fitted line ($y=-0.086\times+1.006$) had an R^2 value of 0.97.

Although phototrophic biomass showed no strong shift within the TIW, one striking difference between our two pairs of samples was that the concentration of low-pigment nanoplankton roughly doubled in terms of abundance and biomass, increasing from an average of 2.2 μg C L^{-1} on the periphery to 4.3 μg C L^{-1} inside the TIW.

While our results showed similar proportions of phagotrophs inside and outside the TIW, the percentage of phagotrophy by high pigment cells decreased from 61% outside the TIW to 40% within the higher nutrient water. We hypothesize that the decreased rates of phagotrophy by high-pigment cells may be a response to increased Fe-input as indicated by the nitrate concentration proxy. Fig. 3 shows a strong negative correlation between the percentage of phagotrophy by high-pigment cells and ambient nitrate concentration ($R^2=0.97$). The relation to nitrate concentration is significant at the 95% confidence level and explains 97% of the variance in ratio of high-pigment to low-pigment phagotrophs. However, it seems unlikely to represent a direct response to nitrate concentration, which should be sufficient for excess N uptake even outside the TIW if cells were not otherwise deficient in Fe.

To further examine the notion that some form of nutrient stress was responsible for the elevated levels of mixotrophy at the stations on the periphery of the TIW, we calculated the NB-S spectral slopes for phagotrophs in each sample (Table 1). The emergent pattern from the four samples indicates that while the size spectra of the low-pigment phagotrophs is uncorrelated with nitrate, the slope of the high-pigment phagotrophs is significantly higher in the lower nutrient water. Thus, high-pigment phagotrophs were larger in size in the lower-nutrient water outside of the TIW.

4. Discussion

4.1. Phototrophs and obligate heterotrophs

Intuitively, one might expect that epifluorescence microscopy can easily differentiate phototrophs from heterotrophs based

Table 1
Station data. Columns are latitude (Lat), longitude (Lon) dissolved nitrate concentration (μM), ,high-pigment and low-pigment nanoplankton (HP and LP, respectively with units of cells mL^{-1}), high-pigment and low-pigment nanoplankton with observable ingested FLB (HP-FLB and LP-FLB, respectively with units of cells mL^{-1}), NB-S slope of the high-pigment phagotrophs (m high), NB-S slope of the low-pigment phagotrophs (m low), natural concentrations of Prochlorococcus (Pro), Synechococcus (Syn), and heterotrophic bacteria (Hbac) (all in cells mL^{-1}) Note that although there is no correlation between the slope of the low-pigment phagotrophs and nitrate, the slope of the high-pigment phagotrophs decreases with increased nutrient loading.

Lat (deg)	Lon (deg)	Nitrate (μM)	HP (cells mL^{-1})	LP (cells mL^{-1})	HP-FLB (cells mL^{-1})	LP-FLB (cells mL^{-1})	m high	m low	Pro (cells mL^{-1})	Syn (cells mL^{-1})	Hbac (cells mL^{-1})
0.5N	123.5W	4.3	1790	590	34	16	0.38	−0.36	$1.71*10^5$	$2.62*10^4$	$8.96*10^5$
1.75N	125W	4.8	1370	480	33	27	0.24	0.17	$1.41*10^5$	$2.40*10^4$	$9.55*10^5$
0.5N	128W	6.4	1460	990	33	25	0.06	−0.28	$3.37*10^5$	$4.33*10^4$	$8.32*10^5$
0.5N	125W	7.8	1460	900	24	36	−0.15	−0.10	$2.98*10^5$	$3.86*10^4$	$9.32*10^5$

solely on the amount of red autofluorescence of cellular chlorophyll. However, we found the probability density function of mean red fluorescence (normalized to exposure time) to be a classic lognormal distribution with no distinct separation between autotrophic and heterotrophic populations (Fig. 4). This unexpected result is due to a strong covariance of chlorophyll fluorescence (red channel of chlorophyll filter) and proflavin fluorescence (green channel of FITC filter) amongst the heterotrophic subset, as shown in Fig. 5, which may be due to either autofluorescence of cellular material other than chlorophyll or a small amount of proflavin fluorescence within the chlorophyll channel. This covariance suggests that for image analysis based community assessments, the ratio of red to green fluorescence should be a more useful diagnostic for distinguishing heterotrophic and phototrophic components of the nanoplankton.

When red:green fluorescence is plotted in log-space, a clear bimodal distribution indicates that the nanoplankton community is comprised of two populations with separate mean ratios (Figs. 1 and 6A). The high red:green fluorescence group is indicative of protists with relatively high chlorophyll content and phototrophic potential while the low red:green fluorescence is indicative of obligate heterotrophs. Fig. 6A shows the probability density function of the logarithm of red to green fluorescence synchronously with a bimodal distribution comprised of two normal

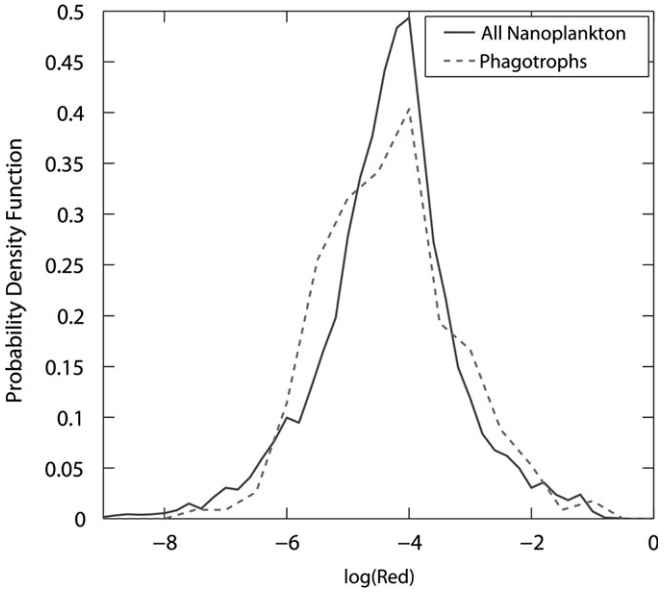

Fig. 4. Probability Density Function (PDF) of the log(red fluorescence) for the entire nanoplankton assemblage (solid line) and for the FLB-ingesting subset (dotted line). Red fluorescence from the chlorophyll channel is normalized to a standard exposure time. Note the log-normal distribution of chlorophyll fluorescence and the striking similarity between the two distributions, suggesting that cellular pigmentation is a poor predictor of phagotrophic behavior.

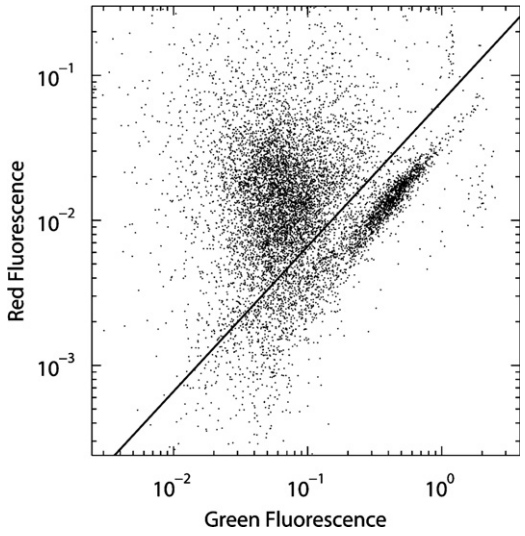

Fig. 5. Densitometric mean red fluorescence of all nanoplankton graphed against densitometric mean green fluorescence (arbitrary units). Fluorescence was normalized by subtracting the mode fluorescence of each image field and dividing by the exposure time. The line denotes the differentiation between high-pigment (phototrophic) and low-pigment (heterotrophic) cells. Note the strong correlation between red and green fluorescence for the heterotrophic subset.

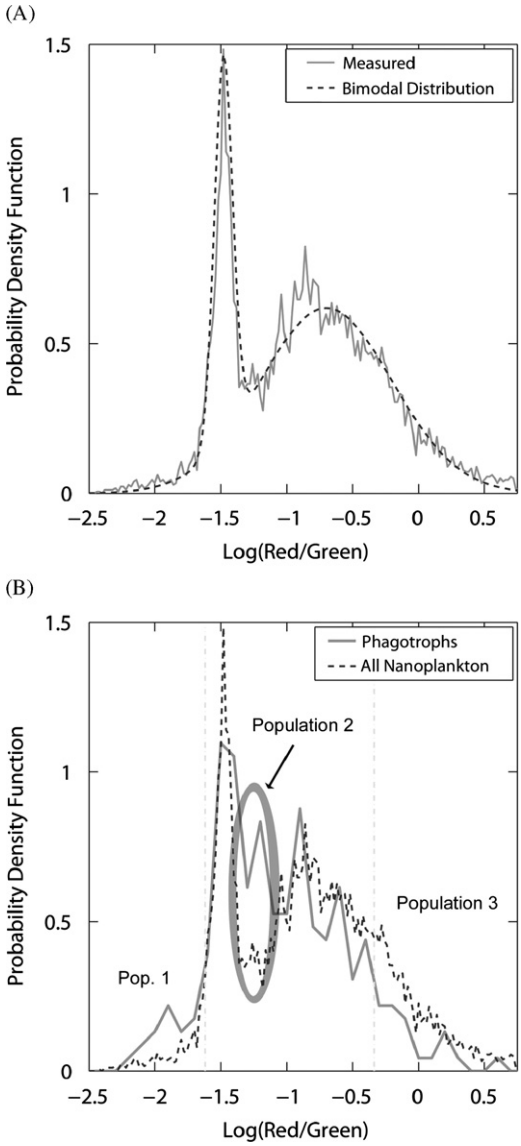

Fig. 6. Probability Density Function (PDF) of the log(red:green fluorescence). Panel A compares the PDF of log(red:green) for all cells to a bi-modal distribution composed of the sum of two normal distributions: obligate heterotrophs ($\mu=-1.48$, S.D.$=0.07$, total number of cells$=2{,}034$) and phototrophs ($\mu=-0.70$, S.D.$=0.5$, total number of cells$=7{,}000$). Panel B compares the PDF of log(red:green) for all cells to the equivalent PDF for the phagotrophic (FLB-ingesting) subset of cells. Three regions of significant difference between the two PDFs were identified. Population 1 is the 5% of cells with the lowest red:green fluorescence and is characterized by an excess concentration of phagotrophs. Population 2 is the transition region from obligate heterotrophs to phototrophs and is also characterized by an excess concentration of phagotrophs. Population 3 is the 20% of cells with the highest red:green fluorescence and is characterized by a deficiency of phagotrophs relative to total cells.

distributions (obligate heterotrophs, $\mu=-1.48$, $\sigma=0.07$; phototrophs, $\mu=-0.80$, $\sigma=0.5$). The large standard deviation of the phototroph fluorescence suggests our low-pigment population is comprised of both obligate heterotrophs and a minor portion of low-chlorophyll phototrophs. Phototrophic cells are thus potentially prone to misclassification as obligate heterotrophs, especially in the region of intermediate red:green fluorescence, making our estimates of the proportions of phototrophs in the total nanoplankton assemblage and phagotrophic subset both conservative. However, as nanophagotrophs consume phototrophs as well as heterotrophic bacteria (Sherr and Sherr, 1992), it is also the case that prior consumption of pigmented prey and gradual degradation of ingested chlorophyll (Strom et al., 1998) may lead to some misclassification of obligate heterotrophs as phototrophs.

Our estimate that 74% of the nanoplankton cells were functionally phototrophic is higher than the vertically integrated ratios for the cruise (60%) and for the 0.5°N transect (53%), as measured microscopically by Taylor et al. (2011). Such a difference is to be expected, however, as our samples were taken in the mixed layer while the proportion of phototrophic biomass typically decreased with depth. Additionally, Taylor et al. (2011) measured a broader size range of organisms including larger heterotrophic dinoflagellates and ciliates that would not have been significantly sampled at our 630X magnification. Our inter-site patterns were consistent with those found by Taylor et al. (2011), with significantly elevated biomass of low-pigment cells within the core of the TIW.

The similarities among the histograms of both red fluorescence (Fig. 4) and red:green fluorescence (Fig. 6B) for all cells and for the FLB-ingesting subset suggests that cellular pigmentation is a poor indicator of phagotrophic functionality. In fact, low-pigment cells (low red:green fluorescence) were only 72% more likely to ingest FLB than high-pigment cells, and the higher cell densities of high-pigment cells resulted in them being responsible for half of the phagotrophy measured.

The above analysis assumes an equal probability of observing an FLB within high-pigment and low-pigment cells. The strong fluorescence of our FLB within the FITC channel indicates that chlorophyll *a* fluorescence was unlikely to mask the FLB signature. The probability of observing an ingested FLB is also related to the digestion time of the phagotrophs. If obligate heterotrophs digest their prey significantly faster than mixotrophs, we may underestimate their relative grazing rates. Sherr et al. (1988) have shown digestion periods for a mixed culture of aplastidic nanoflagellates to be temperature dependent, with digestion periods of ~30 min at high temperature. Although no similar study has measured digestion rates for mixotrophs, it is reasonable to assume from the wide taxonomic distributions of plastidic and aplastidic nanoflagellate phagotrophs that community-averaged digestion rates would not differ appreciably between them.

We have identified three separate populations (Fig. 6B) where chlorophyll fluorescence could be a predictor of phagotrophic potential. Population 1 is composed of extremely low pigmentation cells and hence is likely comprised of only obligate heterotrophs. Population 3 cells, comprising the 20% of the nanoplankton with highest pigmentation, have a relatively low probability of ingesting FLB. Due to the significant Fe-requirements of photosystems, high chlorophyll is often indicative of Fe-sufficiency, and we suspect that these cells are phytoplankton that more easily satisfy their Fe requirements and hence do not need to engage in phagotrophy. Population 2 is composed of cells of intermediate pigmentation. These nanoplankton may be mixotrophs with lower than normal fluorescence and hence a higher need for Fe, or obligate heterotrophs that may have recently ingested a phototroph and had not fully degraded its photosynthetic pigments.

4.2. Mixotrophy in the eastern equatorial Pacific

Although our sample size is modest, the relatively weak dependence of phagotrophic potential on cellular pigmentation suggests that phagotrophy is a ubiquitous trait of both pigmented and non-pigmented nanoplankton in the upper euphotic zone of the EEP. Mixotrophy confers advantages to phytoplankton that are capable of ingesting picoplankton, either to alleviate nutrient deficiencies or to supplement the energy produced by photosynthesis. Jones (2000) divided mixotrophs into four groups. Group A is primarily heterotrophic. Group B is primarily autotrophic but supplements its carbon budget with phagotrophy when light is limiting. Group C supplements its nutrient budget with phagotrophy, and Group D only ingests prey under rare circumstances. The high-pigment phagotrophs assessed in our study must fall into the Group B or C categories of mixotrophs. Group A mixotrophs would have low cellular pigmentation and hence be considered obligate heterotrophs in our assessment. Group D mixotrophs would be unlikely to ingest any FLB. Since our samples came from the 30% light level on clear days at the equator, where phytoplankton instantaneous growth rate was highest and not light limited (Selph et al., 2011), it seems likely that the high-pigment phagotrophs were Group C mixotrophs which ingest prey to alleviate nutrient stress.

Although community grazing rates remained relatively constant throughout the EEP during our study (Selph et al., 2011), heterotrophic biomass was significantly higher within the TIW. Fig. 3 suggests that as mixotrophic grazing pressure decreased at higher nutrient concentrations in this feature, it was replaced by the grazing pressure of obligate heterotrophs. Increased rates of nutrient input in the TIW may therefore have alleviated phototroph nutrient stress and hence decreased their reliance on phagotrophy. If so, this would have the effect of reducing grazing pressure on picoplankton and indirectly diverting more picoplankton production to the obligate heterotrophs.

Maranger et al. (1998) have suggested that ingestion of prokaryotes by mixotrophic flagellates may account for a significant portion of the total Fe uptake of the autotrophic community. As indicated by a dramatic community response in Fe-enrichment experiments (Brzezinski et al., 2011), Fe was the limiting resource during our study. Increased nitrate concentrations inside the TIW point to a higher rate of Fe supply due to enhanced upwelling, while dissolved Fe concentrations remained low inside the TIW, presumably due to rapid incorporation into the planktonic community. Low concentration of Fe would limit the ability of phytoplankton to utilize the excess nitrate brought in by upwelling until Fe became more available by food web cycling or photochemical processes. Thus, by ingestion of nitrogen-rich (and Fe-rich) prey, mixotrophs would require less Fe for synthesis of nitrate reductase. If the correlation between mixotrophy and nitrate as a proxy for phototroph nutrient stress is robust, mixotrophy may be even more prevalent in the lower nutrient waters of oligotrophic regions away from the influence of TIW activity in this area.

Stoecker et al. (1996) examined mixotrophy among micro- and mesoprotozooplankton in the equatorial Pacific, looking for plastids in heterotrophic taxa including ciliates and sarcodines (but excluding dinoflagellates). Evidence of mixotrophy was found for all taxa. According to the classifications of Jones (2000), Stoecker et al. (1996) observed that the larger protists were frequently Group A mixotrophs, which supplement their energy budgets by harboring endosymbionts or engaging in kleptoplastidy. Given the Group C characteristics of nanoflagellates from the present study, the contrasts between these studies suggest a notable size-related difference in the functional roles of mixotrophy among the protists in this region.

4.3. Ecological implications of mixotrophy in HNLC regions

The prevalence of mixotrophy among nanoplankton in the EEP has intriguing implications for the two paradigms that explain sparse phytoplankton communities in HNLC regions: bottom-up Fe-limitation (Behrenfeld et al., 1996) and top-down microzooplankton grazing pressure (Landry et al., 2000a). Widespread phagotrophic behavior of nano-phototrophs induced by nutrient deprivation (whether Fe or N) increases grazing pressure predominantly on picophytoplankton, which dominate abundance and are major contributors to biomass and production (Landry and Kirchman, 2002). The 0.8-μm FLB used in our experiment are meant to serve as a general prey proxy for cells in this size range. This is unlikely to be the case for every population, which may differ substantially in cell surface chemistry, motility, or other factors that affect prey vulnerability to protistan consumers. Nonetheless, previous research using FLBs as tracers in dilution experiments has at least established that grazing rate estimates from FLB disappearance are similar to community grazing rates on cyanobacteria in this region (Landry et al., 1995). In addition, all categories of picophytoplankton showed a strong balance between growth rates and grazing losses to protistan consumers (i.e., microzooplankton grazing) in experiments conducted during our study (Landry et al., 2011).

Although the energy required for phagotrophic phototrophs to synthesize chloroplasts may decrease their maximal growth rate potential (Raven, 1997), energy subsidies from phototrophy allow them to survive at lower prey thresholds than their obligate heterotrophic competitors. The plasticity of the mixotrophic nutritional strategy may therefore contribute to the relative constancy of phytoplankton biomass in the EEP. The phototrophic capability of mixotrophs allows for the decoupling of predator and prey dynamics when prey concentrations are low (e.g. modeling studies by Hammer and Pitchford, 2005; Thingstad et al., 1996). Rather than major predator-prey cycles, maintaining healthy concentrations of mixotrophic nanoflagellates during periods of low prokaryotic production thus conserves grazing potential to crop down picoplankton when their growth rates increase.

In addition to direct grazing impacts, the grazing pressure exerted by mixotrophs may be qualitatively different from that of obligate heterotrophs. Microzooplankton grazing plays a key role in remineralization of nutrients and the maintenance of recycled production in the EEP (Landry et al., 1997). Unlike obligate heterotrophs, which release ammonium and other nutrients while grazing, mixotrophs typically retain most of the nutrients acquired through phagotrophy and hence would not necessarily promote the growth of other phytoplankton, their competitors (Rothhaupt, 1997).

5. Conclusions

The general view that heterotrophic nanoflagellates control the picoplankton community in HNLC regions needs to be amended to include a major role for mixotrophic phytoplankton within the microbial grazing link. Although based on only a few samples, our analysis of phagotrophy in the EEP using FLB indicates that mixotrophy is widespread among nanophytoplankton, consistent with their need for an alternate source of the limiting micronutrient, iron. These phagotrophic phototrophs were responsible for roughly half of the observed ingestion of FLB in our experiments. Unlike obligate heterotrophs, phagotrophy by mixotrophs should be induced only under low-nutrient concentrations, and mixotrophs should retain most of the nutrients acquired from prey rather than contributing to high system recycling. Further work is necessary to assess the roles of mixotrophy in supplying nutrients to nanoflagellates and controlling the growth of not only heterotrophic bacteria but also picophytoplankton populations.

Acknowledgments

We thank the captain and crew of the R.V. *Revelle* for their role in making our work possible. We are also grateful to all of our colleagues on the cruise for their support and collaboration. Special thanks to Mark Hodges, Andrew Taylor, Moira Decima and Dan Wick for help with microscopy; Darcy Taniguchi for assistance with the statistics of nanoplankton size distributions; and Stephen Baines, Ben Twining, and Moira Decima for their insightful comments about our manuscript. This project was supported by the National Science Foundation Grant OCE 0322074 and an NSF Graduate Research Fellowship to M. Stukel.

References

Arenovski, A.L., Lim, E.L., Caron, D.A., 1995. Mixotrophic nanoplankton in oligotrophic surface waters of the Sargasso Sea may employ phagotrophy to obtain major nutrients. Journal of Plankton Research 17, 801–820.

Barber, R.T., Sanderson, M.P., Lindley, S.T., Chai, F., Newton, J., Trees, C.C., Foley, D.G., Chavez, F.P., 1996. Primary productivity and its regulation in the equatorial Pacific during and following the 1991–1992 El Niño. Deep-Sea Research II 43, 933–969.

Baretta-Bekker, J.G., Baretta, J.W., Hansen, A.S., Riemann, B., 1998. An improved model of carbon and nutrient dynamics in the microbial food web in marine enclosures. Aquatic Microbial Ecology 14, 91–108.

Behrenfeld, M.J., Bale, A.J., Kolber, Z.S., Aiken, J., Falkowski, P.G., 1996. Confirmation of iron limitation of phytoplankton photosynthesis in the equatorial Pacific Ocean. Nature 383, 508–511.

Bell, E.M., Laybourn-Parry, J., 2003. Mixotrophy in the Antarctic phytoflagellate, *Pyramimonas gelidicola* (Chlorophyta: Prasinophyceae). Journal of Phycology 39, 644–649.

Brzezinski, M.A., Baines, S., Balch, W.M., Beucher, C., Chai, F., Dugdale, R.C., Krause, J.W., Landry, M.R., Marchi, A., Measures, C.I., Nelson, D.M., Parker, A., Poulton, A., Selph, K.E., Strutton, P., Taylor, A.G., Twining, B.S., 2011. Co-limitation of diatoms by iron and silicic acid in the equatorial Pacific. Deep-Sea Research II 58 (3–4), 493–511.

Calbet, A., Landry, M.R., 1999. Mesozooplankton influences on the microbial food web: Direct and indirect trophic interactions in the oligotrophic open ocean. Limnology and Oceanography 44, 1370–1380.

Caron, D.A., Sanders, R.W., Lim, E.L., Marrase, C., Amaral, L.A., Whitney, S., Aoki, R.B., Porter, K.G., 1993. Light-dependent phagotrophy in the fresh-water mixotrophic chrysophyte *Dinobryon-cylindricum*. Microbial Ecology 25, 93–111.

Coale, K.H., Fitzwater, S.E., Gordon, R.M., Johnson, K.S., Barber, R.T., 1996a. Control of community growth and export production by upwelled iron in the equatorial Pacific Ocean. Nature 379, 621–624.

Coale, K.H., Johnson, K.S., Fitzwater, S.E., Gordon, R.M., Tanner, S., Chavez, F.P., Ferioli, L., Sakamoto, C., Rogers, P., Millero, F., Steinberg, P., Nightingale, P., Cooper, D., Cochlan, W.P., Landry, M.R., Constantinou, J., Rollwagen, G., Trasvina, A., Kudela, R., 1996b. A massive phytoplankton bloom induced by an ecosystem-scale iron fertilization experiment in the equatorial Pacific Ocean. Nature 383, 495–501.

Foley, D.G., Dickey, T.D., McPhaden, M.J., Bidigare, R.R., Lewis, M.R., Barber, R.T., Lindley, S.T., Garside, C., Manov, D.V., McNeil, J.D., 1997. Longwaves and primary productivity variations in the equatorial Pacific at 0°, 140°W. Deep-Sea Research II 44, 1801–1826.

Franck, V.M., Bruland, K.W., Hutchins, D.A., Brzezinski, M.A., 2003. Iron and zinc effects on silicic acid and nitrate uptake kinetics in three high-nutrient, low-chlorophyll (HNLC) regions. Marine Ecology Progress Series 252, 15–33.

Franck, V.M., Smith, G.J., Bruland, K.W., Brzezinski, M.A., 2005. Comparison of size-dependent carbon, nitrate, and silicic acid uptake rates in high- and low-iron waters. Limnology and Oceanography 50, 825–838.

Hammer, A.C., Pitchford, J.W., 2005. The role of mixotrophy in plankton bloom dynamics, and the consequences for productivity. ICES Journal of Marine Science 62, 833–840.

Havskum, H., Hansen, A.S., 1997. Importance of pigmented and colourless nano-sized protists as grazers on nanoplankton in a phosphate-depleted Norwegian fjord and in enclosures. Aquatic Microbial Ecology 12, 139–151.

Jones, R.I., 2000. Mixotrophy in planktonic protists: an overview. Freshwater Biology 45, 219–226.

Jost, C., Lawrence, C.A., Campolongo, F., van de Bund, W., Hill, S., DeAngelis, D.L., 2004. The effects of mixotrophy on the stability and dynamics of a simple planktonic food web model. Theoretical Population Biology 66, 37–51.

Landry, M.R., Barber, R.T., Bidigare, R.R., Chai, F., Coale, K.H., Dam, H.G., Lewis, M.R., Lindley, S.T., McCarthy, J.J., Roman, M.R., Stoecker, D.K., Verity, P.G., White, J.R., 1997. Iron and grazing constraints on primary production in the central equatorial Pacific: an EqPac synthesis. Limnology and Oceanography 42, 405–418.

Landry, M.R., Constantinou, J., Latasa, M., Brown, S.L., Bidigare, R.R., Ondrusek, M.E., 2000a. Biological response to iron fertilization in the eastern equatorial Pacific (IronEx II). III. Dynamics of phytoplankton growth and microzooplankton grazing. Marine Ecology Progress Series 201, 57–72.

Landry, M.R., Kirchman, D.L., 2002. Microbial community structure and variability in the tropical Pacific. Deep-Sea Research II 49, 2669–2693.

Landry, M.R., Kirshtein, J., Constantinou, J., 1995. A refined dilution technique for measuring the community grazing impact of microzooplankton, with experimental tests in the central equatorial Pacific. Marine Ecology Progress Series 120, 53–63.

Landry, M.R., Ondrusek, M.E., Tanner, S.J., Brown, S.L., Constantinou, J., Bidigare, R.R., Coale, K.H., Fitzwater, S., 2000b. Biological response to iron fertilization in the eastern equatorial Pacific (IronEx II). I. Microplankton community abundances and biomass. Marine Ecology Progress Series 201, 27–42.

Landry, M.R., Selph, K.E., Taylor, A.G., Décima, M., Balch, W.M., Bidigare, R.R., 2011. Phytoplankton growth, grazing and production balances in the HNLC equatorial Pacific. Deep-Sea Research II 58 (3–4), 524–535.

Le Borgne, R., Landry, M.R., 2003. EBENE: a JGOFS investigation of plankton variability and trophic interactions in the equatorial Pacific (180°). Journal of Geophysical Research-Oceans 108 (C12), 8136. doi:10.1029/2000JC001252.

Legrand, C., Graneli, E., Carlsson, P., 1998. Induced phagotrophy in the photosynthetic dinoflagellate *Heterocapsa triquetra*. Aquatic Microbial Ecology 15, 65–75.

Maranger, R., Bird, D.F., Price, N.M., 1998. Iron acquisition by photosynthetic marine phytoplankton from ingested bacteria. Nature 396, 248–251.

Martin, E.S., Irigoien, X., Harris, R.P., Lopez-Urrutia, A., Zubkov, M.V., Heywood, J.L., 2006. Variation in the transfer of energy in marine plankton along a productivity gradient in the Atlantic Ocean. Limnology and Oceanography 51, 2084–2091.

Menden-Deuer, S., Lessard, E.J., 2000. Carbon to volume relationships for dinoflagellates, diatoms, and other protist plankton. Limnology and Oceanography 45, 569–579.

Miller, C.B., Frost, B.W., Wheeler, P.A., Landry, M.R., Welschmeyer, N., Powell, T.M., 1991. Ecological dynamics in the Sub-Arctic Pacific, a possibly iron-limited ecosystem. Limnology and Oceanography 36, 1600–1615.

Nygaard, K., Tobiesen, A., 1993. Bacterivory in algae: a survival strategy during nutrient limitation. Limnology and Oceanography 38, 273–279.

Platt, T., Denman, K., 1977. Organization in pelagic ecosystem. Helgolander Wissenschaftliche Meeresuntersuchungen 30, 575–581.

Raven, J.A., 1997. Phagotrophy in phototrophs. Limnology and Oceanography 42, 198–205.

Rothhaupt, K.O., 1997. Nutrient turnover by freshwater bacterivorous flagellates: differences between a heterotrophic and a mixotrophic chrysophyte. Aquatic Microbial Ecology 12, 65–70.

Sabetta, L., Fiocca, A., Margheriti, L., Vignes, F., Basset, A., Mangoni, O., Carrada, G.C., Ruggieri, N., Ianni, C., 2005. Body size-abundance distributions of nano- and micro-phytoplankton guilds in coastal marine ecosystems. Estuarine Coastal and Shelf Science 63, 645–663.

Safi, K.A., Hall, J.A., 1999. Mixotrophic and heterotrophic nanoflagellate grazing in the convergence zone east of New Zealand. Aquatic Microbial Ecology 20, 83–93.

Sanders, R.W., 1991. Mixotrophic protists in marine and fresh-water ecosystems. Journal of Protozoology 38, 76–81.

Sanders, R.W., Berninger, U.G., Lim, E.L., Kemp, P.F., Caron, D.A., 2000. Heterotrophic and mixotrophic nanoplankton predation on picoplankton in the Sargasso Sea and on Georges Bank. Marine Ecology Progress Series 192, 103–118.

Selph, K.E., Landry, M.R., Taylor, A., Yang, E.J., Measures, C.I., Yang, J.J., Stukel, M.R., Christensen, S., Bidigare, R.R., 2011. Spatially-resolved, taxon-specific phytoplankton production and grazing dynamics in relation to iron distributions in the Equatorial Pacific between 110 and 140°W. Deep-Sea Research II 58 (3–4), 358–377.

Sherr, B.F., Sherr, E.B., 1993. Preservation and storage of samples for enumeration of heterotrophic protists. In: Kemp, P.F., Sherr, B.F., Sherr, E.B., Cole, J.J. (Eds.), Handbook of Methods in Aquatic Microbial Ecology. CRC-Press, pp. 207–212.

Sherr, B.F., Sherr, E.B., Fallon, R.D., 1987. Use of monodispersed, fluorescently labeled bacteria to estimate *in situ* protozoan bacterivory. Applied and Environmental Microbiology 53, 958–965.

Sherr, B.F., Sherr, E.B., Rassoulzadegan, F., 1988. Rates of digestion of bacteria by marine phagotrophic protozoa: temperature dependence. Applied and Environmental Microbiology 54, 1091–1095.

Sherr, E.B., Sherr, B.F., 1992. Trophic roles of pelagic protists: phagotrophic flagellates as herbivores. Archiv für Hydrobiologie, Beiheft Ergebnisse der Limnologie 37, 165–172.

Sherr, E.B., Sherr, B.F., 2002. Significance of predation by protists in aquatic microbial food webs. Antonie Van Leeuwenhoek International Journal of General and Molecular Microbiology 81, 293–308.

Stoecker, D.K., Gustafson, D.E., Verity, P.G., 1996. Micro- and mesoprotozooplankton at 140°W in the equatorial Pacific: heterotrophs and mixotrophs. Aquatic Microbial Ecology 10, 273–282.

Strom, S.L., Morello, T.A., Bright, K.J., 1998. Protozoan size influences algal pigment degradation during grazing. Marine Ecology Progress Series 164, 189–197.

Strutton, P.G., Palacz, A.P., Dugdale, R.C., Chai, F., Marchi, A., Parker, A.E., Hogue, V., Wilkerson, F.P., 2011. The impact of equatorial Pacific tropical instability waves on hydrography and nutrients: 2004–2005. Deep-Sea Research II 58 (3–4), 284–295.

Strutton, P.G., Ryan, J.P., Chavez, F.P., 2001. Enhanced chlorophyll associated with tropical instability waves in the equatorial Pacific. Geophysical Research Letters 28, 2005–2008.

Taylor, A.G., Landry, M.R., Selph, K.E., Yang, E.J., 2011. Biomass, size structure and depth distributions of the microbial community in the eastern equatorial Pacific. Deep-Sea Research II 58 (3–4), 342–357.

Thingstad, T.F., Havskum, H., Garde, K., Riemann, B., 1996. On the strategy of "eating your competitor": a mathematical analysis of algal mixotrophy. Ecology 77, 2108–2118.

Unrein, F., Massana, R., Alonso-Saez, L., Gasol, J.M., 2007. Significant year-round effect of small mixotrophic flagellates on bacterioplankton in an oligotrophic coastal system. Limnology and Oceanography 52, 456–469.

Zubkov, M.V., Tarran, G.A., 2008. High bacterivory by the smallest phytoplankton in the North Atlantic Ocean. Nature 455, 224–248.